The Canadian Mineralogist
Vol. 36, pp. 117-135 (1998)

COMPOSITION OF CHROMITE IN THE UPPER CHROMITITE, MUSKOX LAYERED INTRUSION, NORTHWEST TERRITORIES

THOMAS A. ROACH AND PETER L. ROEDER[1]

Department of Geological Sciences, Queen's University, Kingston, Ontario K7L 3N6

LARRY J. HULBERT

Geological Survey of Canada, 601 Booth Street, Ottawa, Ontario K1A 0E8

ABSTRACT

The texture, mineralogy and composition of chromite in the upper chromitite of the Muskox intrusion, in the Northwest Territories, have been studied in two 0.5-meter sections of drill core. The principal rock-type is an orthopyroxenite that contains cumulus olivine, orthopyroxene and chromite, and the intercumulus minerals clinopyroxene and plagioclase. The minor minerals ilmenite and biotite are found, together with a number of accessory minerals, in pockets that are interpreted as sites of late intercumulus melt. The chromitite seam is up to 10 cm thick and contains chromite with a narrow range in composition: $0.64 < Cr/(Cr + Al) < 0.74$, $0.62 < Fe^{2+}/(Fe^{2+} + Mg) < 0.69$, and $0.18 < Fe^{3+}/(Fe^{3+} + Al + Cr) < 0.26$. The average composition of chromite in the chromitite, and the olivine and orthopyroxene in the orthopyroxenite, were used to calculate a temperature of 1146°C and $\log f(O_2) = -9.1$. The disseminated chromite in the orthopyroxenite shows a much greater range in composition, and increases in $Fe^{2+}/(Fe^{2+} + Mg)$, $Fe^{3+}/(Fe^{3+} + Al + Cr)$, Ti and Ni with stratigraphic height above the massive chromitite. The chromite in the Muskox chromitite is significantly higher in Fe^{3+}, Ti and $Fe^{2+}/(Fe^{2+} + Mg)$ than chromite in the Bushveld, Stillwater and Great Dyke chromitites; furthermore, the Muskox chromitites formed much higher in the stratigraphic section of the layered series than in these other intrusions. The Muskox chromitites are considered to have formed late in the magmatic history of the intrusion as a result of mixing of a fractionated magma with a more primitive magma and a component due to wall-rock assimilation.

Keywords: chromite, chromitite, orthopyroxene, layered intrusions, Muskox, Northwest Territories.

SOMMAIRE

Nous avons étudié la texture et la composition de la chromite qui constitue la chromitite supérieure du complexe intrusif de Muskox, dans les Territoires du Nord-Ouest, en utilisant deux sections de carottes, chacune de 0.5 mètres de longueur. La roche encaissante est principalement une orthopyroxénite contenant olivine, orthopyroxène et chromite cumulatives, ainsi que les minéraux intercumulus clinopyroxène et plagioclase. Les minéraux accessoires ilménite et biotite coexistent avec quelques autres minéraux plus rares dans des poches que nous interprétons comme sites de magma intercumulus tardif. La couche de chromitite atteint une épaisseur de 10 cm, et la chromite y possède un intervalle étroit de composition: $0.64 < Cr/(Cr + Al) < 0.74$, $0.62 < Fe^{2+}/(Fe^{2+} + Mg) < 0.69$, et $0.18 < Fe^{3+}/(Fe^{3+} + Al + Cr) < 0.26$. La composition moyenne de la chromite dans la chromitite, et celle de l'olivine et de l'orthopyroxène dans l'orthopyroxénite, ont servi pour calculer la température, 1146°C, et la fugacité de l'oxygène, $\log f(O_2) = -9.1$. En revanche, la chromite disséminée dans l'orthopyroxénite montre un intervalle beaucoup plus grand de valeurs de $Fe^{2+}/(Fe^{2+} + Mg)$ et de $Fe^{3+}/(Fe^{3+} + Al + Cr)$, et des teneurs plus élevées en Ti et Ni selon l'élévation stratigraphique au dessus de la chromitite massive. La chromite de la chromitite de Muskox est nettement plus riche en Fe^{3+} et Ti, et possède un rapport $Fe^{2+}/(Fe^{2+} + Mg)$ plus élevé, que la chromite des chromitites des complexes de Bushveld, Stillwater et Great Dyke; de plus, à Muskox, les niveaux de chromitite se sont formées beaucoup plus haut dans la section stratigraphique que dans ces autres complexes intrusifs. A Muskox, les chromitites se seraient formées tardivement au cours de l'évolution magmatique suite à un mélange de magma fractionné avec un magma plus primitif et un composant contaminé par assimilation des roches encaissantes.

(Traduit par la Rédaction)

Mots-clés: chromite, chromitite, orthopyroxène, complexes stratiformes, Muskox, Territoires du Nord-Ouest.

[1] To whom correspondence should be addressed. *E-mail address*: roeder@geolserv.geol.queensu.ca

Introduction

Horizons of chromitite are prominent in the sequence of cumulates in the Muskox layered intrusion, located south of the Coronation Gulf in the Northwest Territories (Fig. 1). The emplacement of the Muskox intrusion is considered to be synchronous at about 1270 Ma with the Coppermine River volcanic rocks to the north and the Mackenzie dyke swarm (LeCheminant & Heaman 1989). The narrow dyke south of the Coppermine River is considered by most investigators to be a feeder dyke that broadens into the funnel-shaped Muskox intrusion north of the Coppermine River. The layers of the intrusion dip to the north and disappear under cover rocks. A large gravity and magnetic anomaly to the north of the intrusion suggests (Irvine & Baragar 1972) that the present outcrop of the Muskox intrusion represents only a small portion of the whole intrusion. The purpose of the present contribution is to characterize the texture and composition of the chromite associated with the upper chromitite.

Background Information

The intrusion was mapped by Smith (1962) and Smith *et al.* (1963) and divided by Irvine & Smith (1969) into two marginal groups, a layered series and granophyric roof-zone. The layered series of the intrusion is about 1800 m thick and is comprised of 42 mappable units of 18 different rock-types. These units dip gently to the north at about 5–8° and have been divided into 25 cyclic units. Each of these cyclic units was interpreted by Irvine & Smith (1967) and Irvine (1970) as due to the influx of a new pulse of magma into the intrusion. The order of crystallization of the major silicates in these cyclic units is variable, and changes with height above the base (Fig. 2). Irvine (1970) divided the layered series into three classes based upon the sequence of crystallizing phases. The crystallization sequence (Class I) for much of the Muskox intrusion involved olivine as the first phase, followed by clinopyroxene, plagioclase, and then orthopyroxene. Higher in the layered series, the orthopyroxene appears earlier as a definite cumulus phase and follows olivine (Class III) near the top of the layered series (Fig. 2). Chromite occurs through much of the layered series (Irvine 1975) as a minor disseminated phase (1–3%). The correlation of whole-rock nickel with the amount of chromite suggests that chromite and olivine coprecipitated (Irvine 1975). The only significant layers of chromitite occur at the base of cyclic units 21 and 22, which are three quarters of the way up the layered series (Fig. 2). Francis (1994) combined the twenty-five cyclic units described by Irvine and Smith into four megacycles that are consistent with the original mapping conducted by Smith *et al.* (1963). The layer containing chromitite described in the present study is at the base of cyclic unit 22, which is near the bottom of megacycle 4. This is in the part of the layered series where orthopyroxene becomes an important cumulus phase, and where DesRoches (1992) and Francis (1994) found geochemical evidence, from elevated ratios of large-ion-lithophile (LIL) to high-field-strength (HFS) elements, that there was enhanced contamination of the magma by crust (Irvine 1970). This contamination may have resulted from roof melting, which increased the silica activity sufficiently to cause orthopyroxene to become a major liquidus phase.

The chromitites in cyclic units 21 and 22 are both situated above layers of peridotite and below orthopyroxenite (Irvine 1975), although the amount of peridotite in cyclic unit 22 is small. There is only a limited amount of published chemical data on the chromite in these two horizons (Irvine 1967). We undertook this study in order to describe the upper chromitite at the base of cyclic unit 22 and to present compositional data on chromite associated with the chromitite and dissenminated in orthopyroxenite. The samples were taken from a half-meter section of two drill cores (MX3 and MX4) that intersect this horizon. Their location is shown on Figure 1 by the numbers 3 (MX3) and 4 (MX4).

Analytical Procedure

All mineral analyses were performed on polished thin sections using an Applied Research Laboratories SEMQ Electron Microprobe in the Department of Geological Sciences at Queen's University. The minerals were analyzed using energy-dispersion spectrometry at 15 kV and a beam current of approximately 20 nA. The standards included glass from the National Bureau of Standards (NBS 470 K412), chromite from Tiebaghi (USNM 117075), and olivine (USNM 2566) provided by the Smithsonian Institution. Corrections were made using the procedure of Bence & Albee (1968) and the alpha corrections of Albee & Ray (1970). The proportion of Fe^{2+} and Fe^{3+} in the chromite was calculated assuming a stoichiometric spinel structure. Seven chromite standards were analyzed a number of times, and the secondary standard closest in composition to the Muskox chromite was analyzed thirteen times. The results of these analyses and a more complete description of the analytical procedures are given by Roach (1992).

Petrography and Mineralogy

The focus of the petrographic examination was to ascertain the relationship between chromite and silicates in the layer that contains chromitite. Figures 3 and 4 illustrate the variation in rock type and composition of chromite within the half-meter interval of the MX3 and MX4 drill core. These samples are from within Class III of Irvine (1970), where the silicate

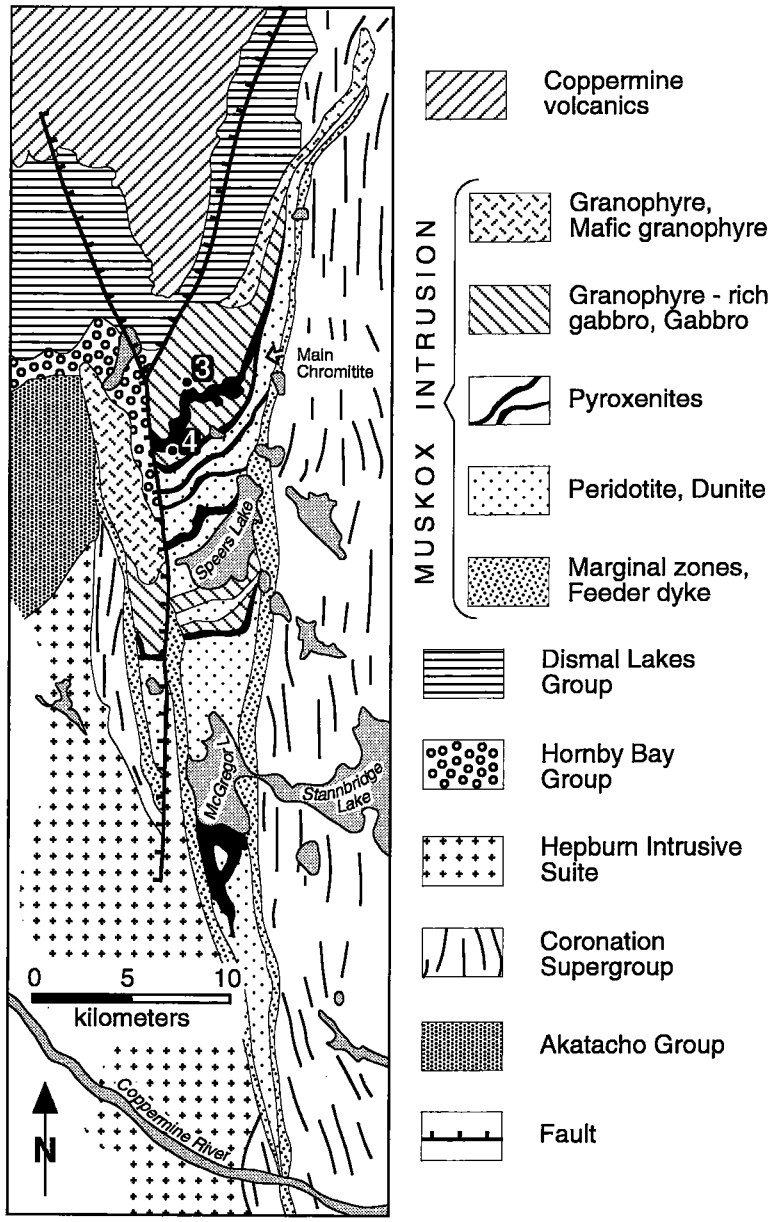

FIG. 1. Generalized geological map of the Muskox intrusion (Irvine & Smith 1969, Hoffman 1984). The drill core used in the present study was taken from the locations labeled "3" (MX3) and "4" (MX4).

crystallization-sequence is thought to be olivine – orthopyroxene – clinopyroxene – plagioclase.

The principal rock-type in the two sections is medium-grained orthopyroxenite that contains euhedral to subhedral orthopyroxene, with up to 20% olivine and variable amounts of chromite, clinopyroxene and plagioclase. The other major rock-type in these sections is chromitite, defined as bands or stringers, >2 mm thick, having greater than 30% by volume of chromite. The orthopyroxenite below or associated with the chromitite is coarse grained, verging on pegmatite. The orthopyroxene, olivine and chromite are interpreted in

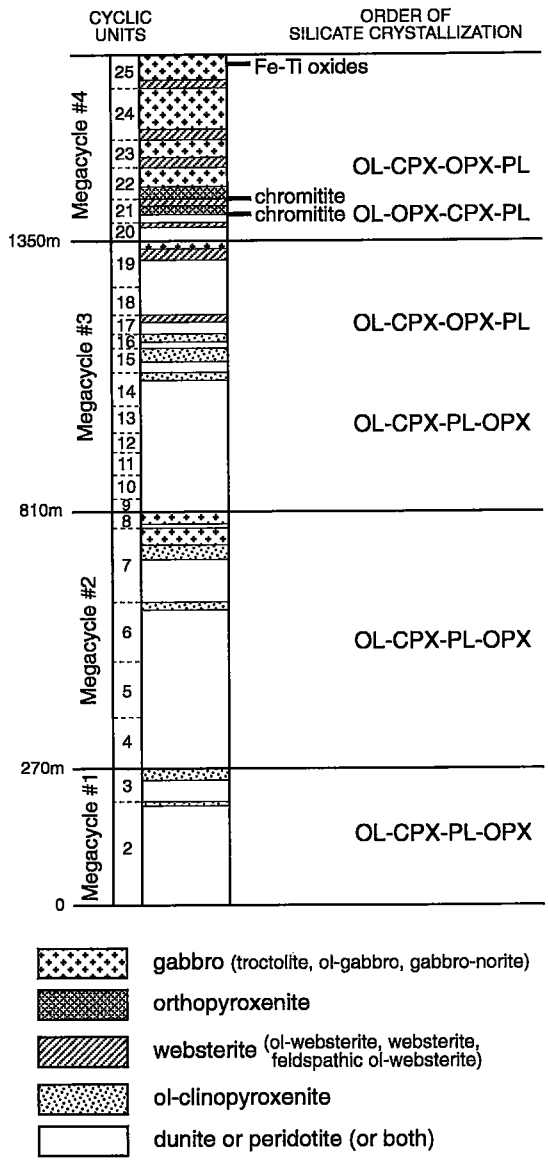

FIG. 2. Summary of Muskox cyclic units and megacycles. Adapted from DesRoches (1992) and Francis (1994).

these sections as cumulus minerals, using the definition of cumulus of Irvine (1982). Orthopyroxene has been interpreted both as the major cumulus mineral in the two sections and a major intercumulus mineral. Orthopyroxene commonly develops at the expense of olivine, leaving rounded or embayed aggregates, which have altered to a mixture of talc and serpentine (Fig. 5). Orthopyroxene grains have euhedral terminations where in contact with plagioclase (Fig. 6), but anhedral where intergrown with other orthopyroxene and clinopyroxene. This texture is similar to that of pyroxenite associated with the UG2 chromitite in the Bushveld Complex (Cawthorn & Barry 1992) and that for the ultramafic zone of the Stillwater intrusion (Jackson 1961).

Chromite

The mode of occurrence of chromite is classified as either massive, in chromitites, or disseminated, in orthopyroxenite. The disseminated grains are usually equant and fairly evenly distributed; however, in zones containing significant modal olivine, ilmenite, and biotite, chromite grains tend to be less regular in shape and to cluster together, forming larger anhedral aggregates. Figure 7 illustrates a sample of orthopyroxenite and best represents typical disseminated chromite. The individual grains are euhedral, less than 0.25 mm in diameter, and associated with cumulus orthopyroxene. Figure 8 is an example of a highly fractured olivine orthopyroxenite. Note that the chromite grains are commonly clustered in aggregates between olivine grains, rather than enclosed within them. The anhedral aggregates of chromite are considered to result from sintering of several small but separate grains (Hulbert & von Gruenewaldt 1985) and may represent the location of pockets of late intercumulus melt (Roeder & Campbell 1985). There are all gradations between separate disseminated grains to large amoeboid grains that are, in some instances, surrounded by biotite.

Orthopyroxenite that contains disseminated chromite grades within a few millimeters to chromitite (Fig. 9). The MX4 section contains a number of irregular, wispy stringers of chromitite, one of which is seen in the center of Figure 9, just above a more massive chromitite. The main chromitite from MX4 (depth interval 29–38 cm) contains chromite evenly distributed in a matrix of large poikilitic crystals of pyroxene and plagioclase. Some pyroxene or plagioclase oikocrysts can contain, in the plane of the thin section, hundreds of chromite grains. Characteristically, the chromite grains in the chromitite are not uniform in size (Fig. 10). Chromite is noticeably larger in plagioclase and along the boundaries of oikocrystic grains. These larger chromite grains are attributed to recrystallization of smaller grains along silicate grain boundaries in the presence of a small amount of late interstitial melt. The difference in size between chromite in clinopyroxene oikocrysts and that in adjoining plagioclase oikocrysts suggests that the larger grains of chromite in plagioclase were enclosed at a later time, but still in the presence of melt.

The massive chromitite grades upward into chromitite that contains a few chromite-free areas (Fig. 10) and, at a higher level, into a chromitite with many irregular chromite-free areas that give the chromitite a somewhat mottled appearance (not shown). The chromite-free areas are 1–3 mm in length

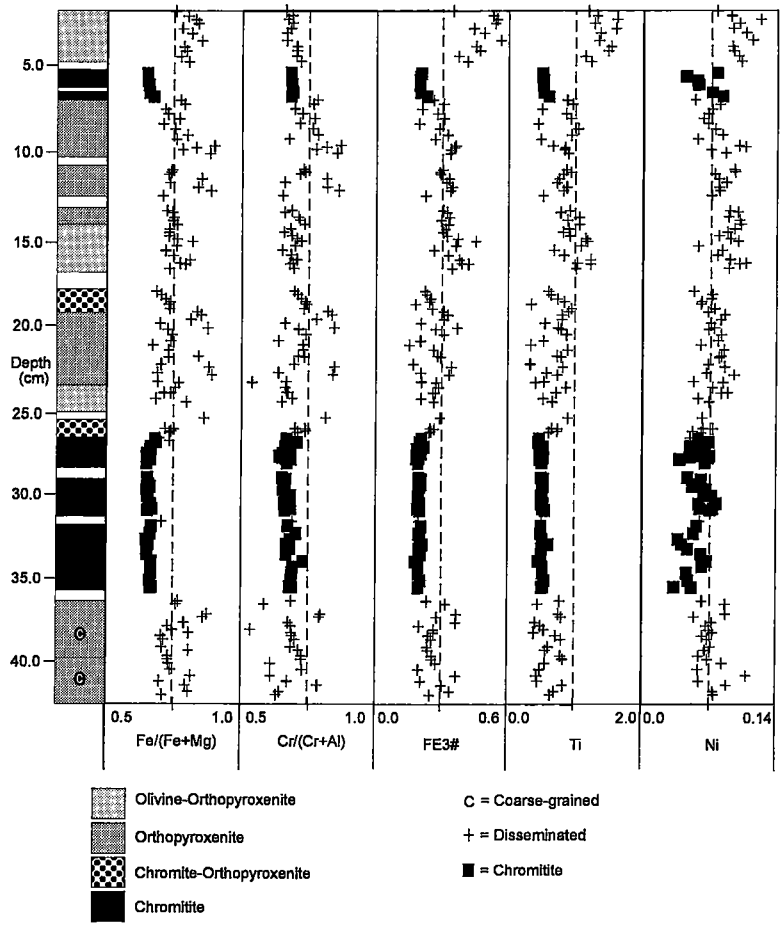

FIG. 3. Rock types and chemical composition of chromite, MX3 drillcore. Depth below drill collar is 56.01 meters plus listed depth in centimeters. Blank areas in section represents missing core. FE3# = $Fe^{3+}/(Fe^{3+} + Al + Cr)$. Ti and Ni as cations per 24 atoms of oxygen.

and are mainly filled by orthopyroxene and clinopyroxene. These chromite-free areas commonly contain small anhedral grains of olivine or orthopyroxene (right side of Fig. 11) that are interpreted as relict cumulus grains. The clinopyroxene in the chromite-free areas generally extends well beyond the chromite-free area as a single-crystal oikocryst (Fig. 11) containing many chromite grains. Some of these chromite-free areas are flattened parallel to igneous layering, with a well-defined ovoid shape (Fig. 10); others are much less regular in outline. Despite the differences in shape, these features seem to have resulted from a similar process. Features such as these were noted in the Stillwater Complex by Jackson (1961) and in the Bushveld complex by Eales & Reynolds (1986), and have been attributed to the replacement of cumulus orthopyroxene and olivine, and to retention of the original cumulus distribution of chromite.

Most chromite in chromitite is found as discrete grains with a euhedral to subhedral, equant habit. Grains have an average diameter of 0.1 mm with a maximum diameter of about 0.5 mm. The majority of the chromite grains are enclosed within silicates other than olivine, and indeed chromite seems to be sparse in olivine. Those grains enclosed in olivine or cumulus orthopyroxene are generally small (<0.1 mm). This is expected, as chromite was an early cumulus phase

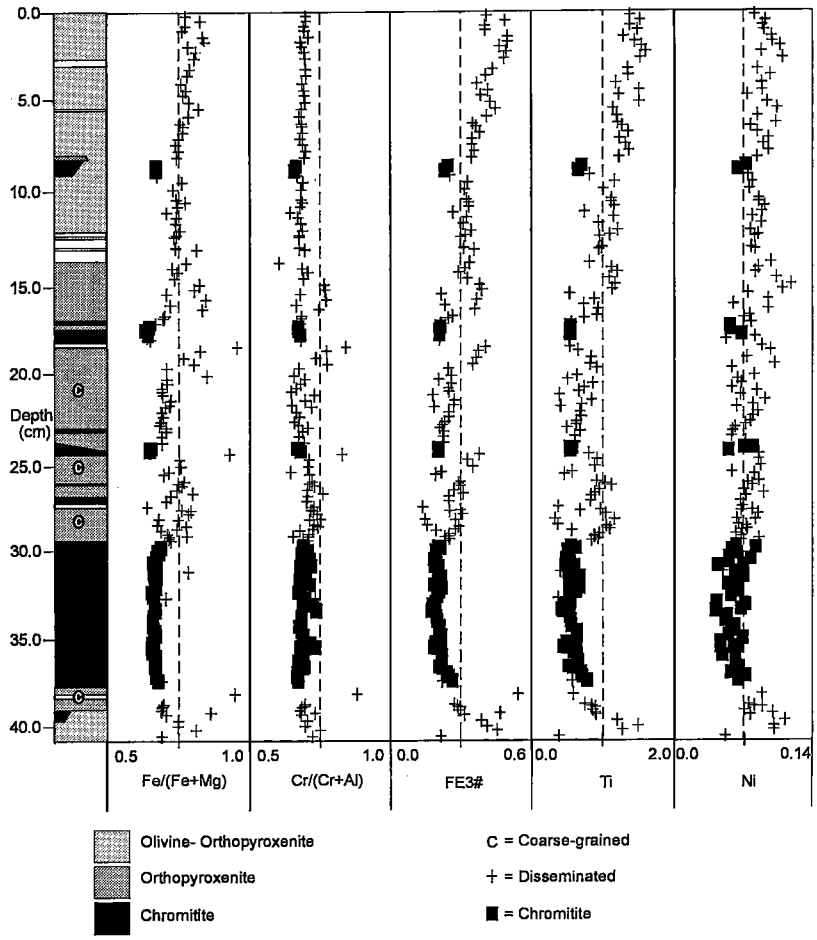

FIG. 4. Rock types and chemical composition of chromite, MX4 drillcore. Depth below drill collar is 95.64 meters plus listed depth in centimeters. Blank areas in section represents missing core. FE3# = $Fe^{3+}/(Fe^{3+} + Al + Cr)$.

whose growth would be restricted after enclosure by other early phases such as olivine or orthopyroxene. In contrast, chromite found in plagioclase, the latest major postcumulus phase, is generally larger (up to 0.5 mm). Some of the larger grains of chromite are irregular in outline, but crystal faces can be identified in the outline. These grains seem as though they are aggregates of many small crystals that have partially recrystallized, and or sintered, into a larger grain.

Olivine

Olivine, a relatively minor modal constituent, occurs in a variety of different habits and associations. Typical olivine and its alteration products make up 10–20% of rocks designated olivine orthopyroxenite and less than 10% in orthopyroxenite. Some samples contain alternating laminae of olivine orthopyroxenite and orthopyroxenite a few millimeters thick (Fig. 8). Alteration of olivine is heterogeneously developed; in areas that contain significant olivine, partial replacement by serpentine is the most common type of alteration. Serpentinization and volume change have produced pervasive fractures in the olivine orthopyroxenite laminae that are nearly parallel to igneous layering. The fractures that extend through pyroxene or plagioclase do not contain alteration products.

The olivine grains in olivine orthopyroxenite are typically euhedral to subhedral, with an average diameter of 0.75 mm, and a maximum diameter of 2 mm

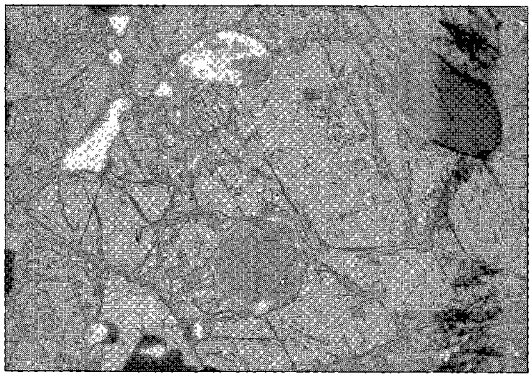

FIG. 5. Orthopyroxene surrounding areas containing a mixture of serpentine and talc. Slide MX–303 (depth 5–9 cm). Width of field of view: 1.8 mm.

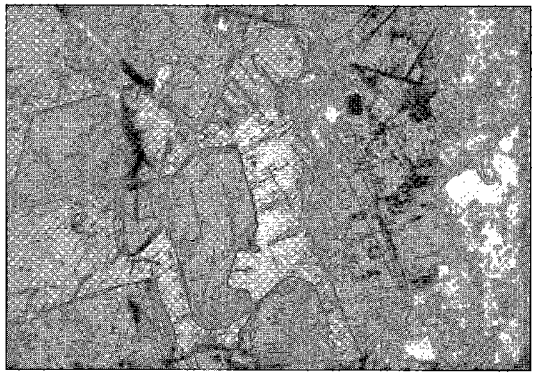

FIG. 6. Orthopyroxene crystals in a matrix of clear plagioclase. Width of field of view: 1.8 mm.

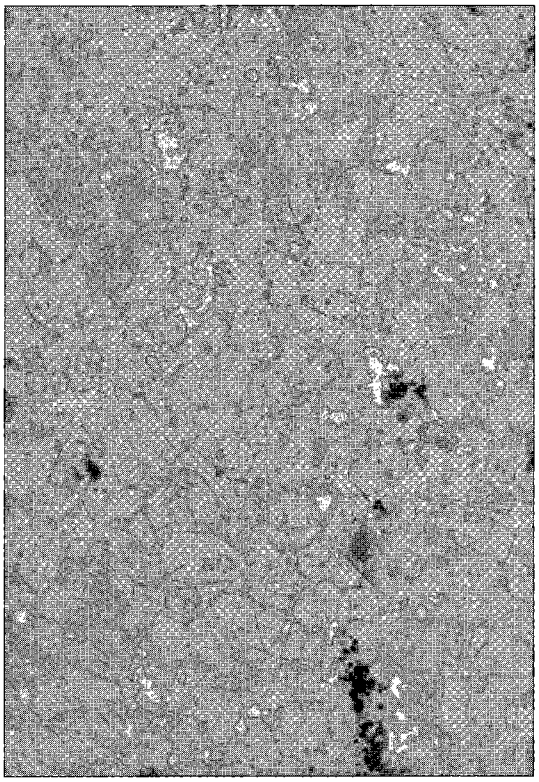

FIG. 7. Orthopyroxenite with intercumulus plagioclase (clear) and disseminated opaque grains of chromite. Slide MX–303 (depth 5–9 cm). Width of field of view: 9.3 mm.

(Fig. 12). Both olivine and orthopyroxene exhibit good cumulus textures. Some orthopyroxene contains small (<0.5 mm), rounded, fine-grained aggregates enclosed within the pyroxene (Fig. 5) that have a composition (No. 6, Table 1) between that of talc and serpentine. This composition is close to that reported by Worden *et al.* (1991) for intimately intergrown talc and serpentine. The olivine associated with coarse-grained orthopyroxenite may be quite large (up to 5 mm) and has a rounded morphology suggestive of reaction.

The composition of most of the olivine in the orthopyroxenite shows little variation. The average result of twenty analyses of olivine from MX3 and MX4 is $Fo_{76.7}$ (SD = 1.0). Olivine located close to pockets that contained late-intercumulus melt may be more fayalitic (No. 5, Table 1).

Orthopyroxene and clinopyroxene

Orthopyroxene is the dominant phase in both MX3 and MX4 and is commonly associated with minor clinopyroxene. Orthopyroxene is generally cumulus, with associated post-cumulus overgrowth; on the other hand, clinopyroxene is of postcumulus origin. There is considerable variation in grain size and texture of pyroxene. Orthopyroxenite above the chromitite has equant orthopyroxene, 0.25–0.30 mm in diameter, that varies from euhedral (Fig. 6) where in contact with plagioclase to anhedral grains where in contact with other silicates. Orthopyroxene grains contain exsolution lamellae of clinopyroxene, and some orthopyroxene contains rounded blebs of clinopyroxene that are less calcic than the discrete grains of clinopyroxene (Roach 1992).

The grains of clinopyroxene are generally smaller than the associated grains of orthopyroxene, except in some coarse-grained orthopyroxenite or chromitite; the clinopyroxene grains contain exsolution lamellae. Oikocrysts of clinopyroxene up to 5 mm across are typically the most abundant intercumulus phase in the more massive part of the chromitite (Fig. 11). The upward transition from more massive chromitite to

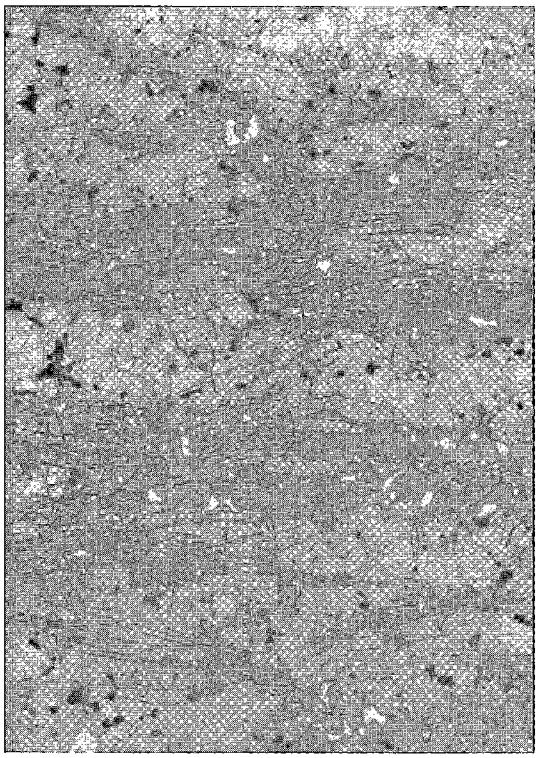

FIG. 8. Disseminated chromite in alternating laminae of orthopyroxenite and olivine orthopyroxenite. The olivine orthopyroxenite contains serpentinized and fractured olivine. Slide MX–404 (depth 10–12 cm). Width of field of view: 10.8 mm.

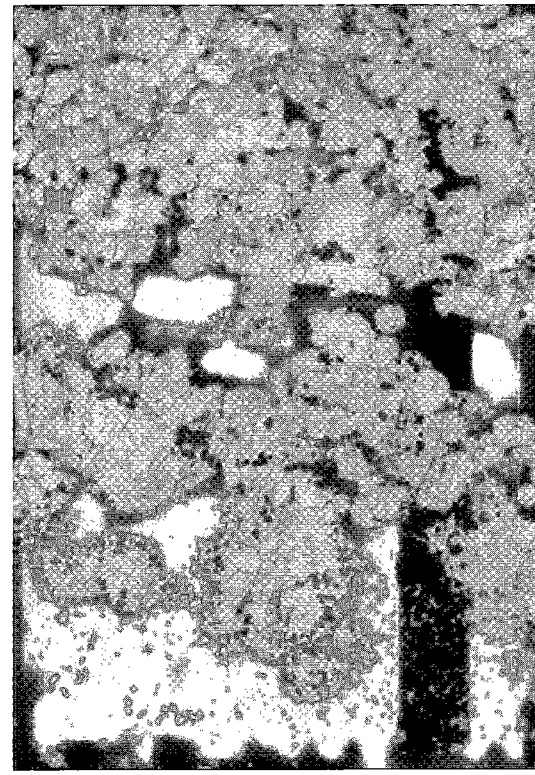

FIG. 9. Orthopyroxenite with wispy layer of chromitite (center) and more massive chromitite (bottom). Slide MX–407 (depth 14–19 cm). Width of field of view: 9.9 mm.

chromitite with irregular chromite-free areas is marked by the upward appearance of orthopyroxene as a significant intercumulus phase, as well as of relict cumulus olivine.

Representative results of analyses of orthopyroxene and clinopyroxene are given in Table 1. Coexisting orthopyroxene and clinopyroxene in ten different samples have a narrow range in $Fe^{2+}/(Fe^{2+} + Mg)$, but variable level of Ca. The average composition (standard deviation in parentheses) of the orthopyroxene in terms of wollastonite, enstatite and ferrosilite is $Wo_{4(0.3)}En_{75(0.6)}Fs_{21(0.7)}$ and that of the clinopyroxene is $Wo_{37(5)}En_{51(3)}Fs_{12(2)}$. Part of the variability in measured calcium for the clinopyroxene is believed to be due to the variable size and distribution of the exsolution lamellae relative to the size and position of the electron beam during analysis.

Plagioclase

Plagioclase is generally the last major intercumulus phase to crystallize; the morphology of the crystals is almost completely controlled by the shape of the interstices remaining among the other phases (Fig. 6). In the lower part of the two sections, plagioclase is volumetrically less abundant than clinopyroxene, but the amount of plagioclase seems to increase toward the top of both sections, where it is more abundant than clinopyroxene. Typical plagioclase grains show twinning and vary in composition from An_{60} to An_{50}.

Accessory minerals in pockets

There are a number of discrete patches that contain a mixture of biotite, ilmenite, chromite, chlorite and minor minerals such as pectolite, apatite, rutile (No. 13, Table 1), armalcolite (No. 14, Table 1), hematite (No. 10, Table 1), monazite, Fe–Ni–Cu sulfides, baddeleyite and alkali feldspar. One good example, shown by the arrow in Figure 12 and enlarged in Figure 13, is taken from 100 cm below the massive chromitite in MX3. This patch is enclosed by olivine in the plane of the thin section (Fig. 13), whereas the much larger patch shown in Figure 14 is bounded by olivine, pyroxene

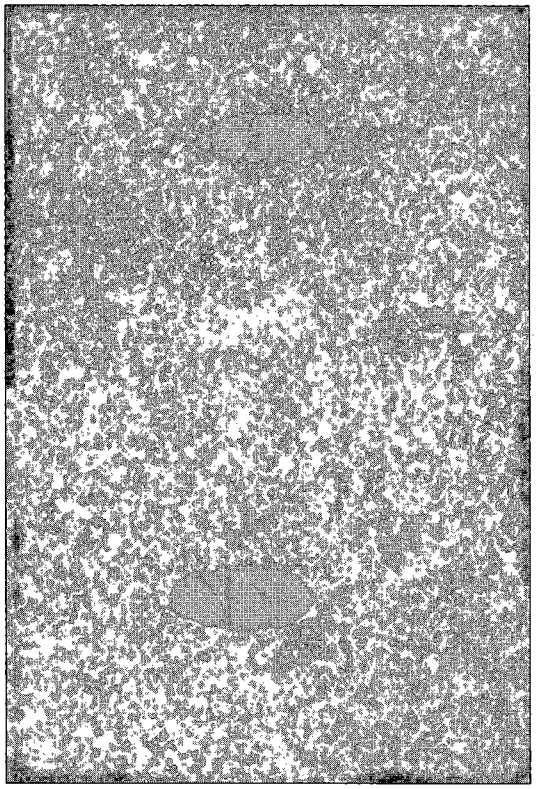

FIG. 10. Chromitite with two chromite-free areas of clinopyroxene and orthopyroxene. Slide MX–410B (depth 31–34 cm). Width of field of view: 11.6 mm.

and plagioclase. The position of some of the labels for the minerals in Figures 13–15 indicate the location of the spots analyzed (data given in Table 1). These patches of accessory minerals are very similar to those found by Roeder & Campbell (1985) in the Jimberlana intrusion and by Hanski (1992) in olivine from the Pechenga ferropicrite. In both cases, these were interpreted as the sites of late interstitial melt. The major silicates are commonly zoned in the vicinity of these patches; for example, plagioclase of composition An_{60-50} may be zoned to almost pure albite, and some grains of pyroxene look ragged in the vicinity of these patches.

Ilmenite, a minor phase in the orthopyroxenites, increases in modal abundance toward the top of both sections. This distribution parallels the overall upward increase of Ti in chromite and the greater modal abundance of associated pale to deep brown, pleochroic biotite that contains 2 to 8 wt.% TiO_2. The biotite commonly surrounds large anhedral grains of ilmenite (Fig. 14). The ilmenite shown in Figures 14 and 15 is separated from the biotite by a rim of hematite that is connected to plates of hematite that extend into biotite. Another example of the complex assemblage of oxide minerals found in some samples is shown in Figure 16 where ilmenite, rutile and armalcolite are in contact with a large grain of chromite. The compositions of these oxides are given in Table 1 (No. 12–15). The composition of armalcolite is consistent with the definition given by Bowles (1988) and is similar, except for higher Cr and Ca, to that reported in experimental runs by Cawthorn & Biggar (1993). Their experiments were designed to test the crystallization of armalcolite,

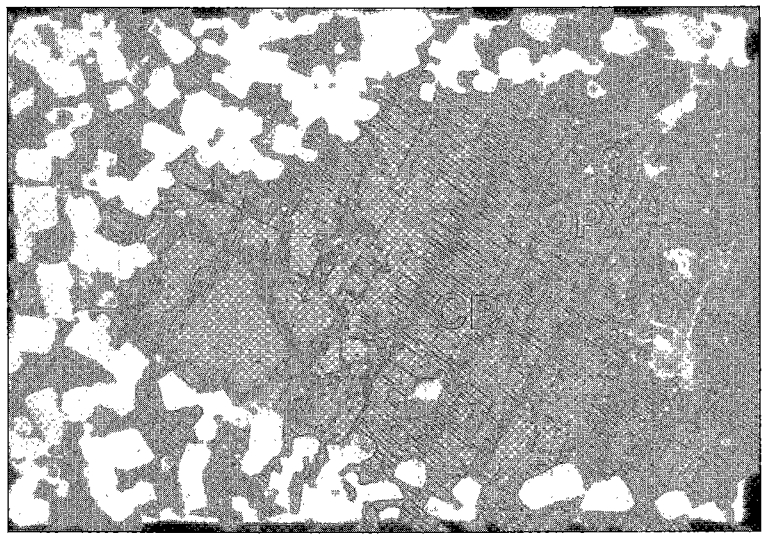

FIG. 11. Enlarged view of the left-hand part of the upper chromite-free area in Figure 10. Large oikocryst of clinopyroxene with good cleavage encloses many crystals of chromite. Slide MX–410B (depth 31–34 cm). Width of field of view: 1.5 mm.

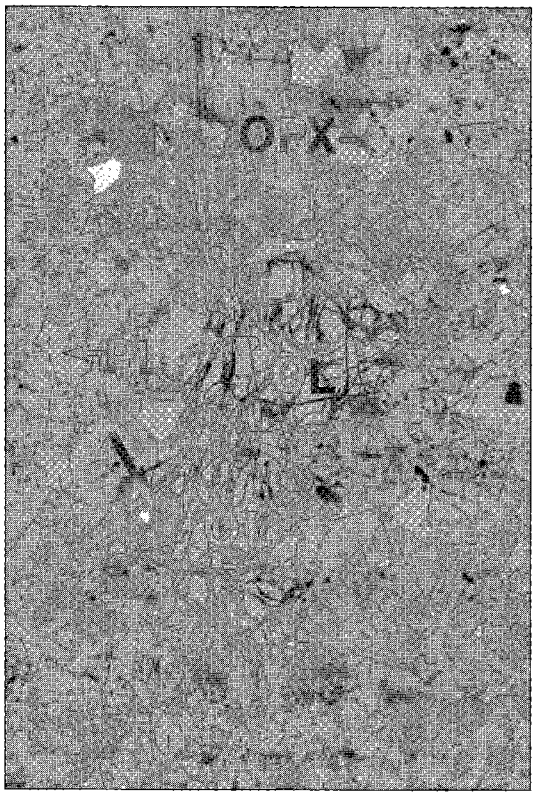

FIG. 12. Orthopyroxenite with two large grains of olivine, one above the other. Arrow without label indicates a mineral assemblage within the lower crystal that may have formed from late intercumulus melt. See Figure 13 for a more detailed view of this area. Slide MX–332B (depth 126–132 cm). Width of field of view: 4.6 mm.

titanium-rich chromite and ilmenite in titanium-rich magma, such as that involved in the Mount Ayliff intrusion in South Africa.

CHEMICAL COMPOSITION OF CHROMITE

Representative results of chemical analyses of chromite are given in Table 2. Figures 3 and 4 display the correlation between the element ratios of chromite and the rock type for each of the two drill-cores. The chromite in chromitite bands shows little chemical variation within, or among bands, and is similar in MX3 and MX4. There is no significant compositional variation of the chromite in the chromitite related to stratigraphic height. The chromite in the chromitite likely represents the closest approach to primary magmatic chromite.

The disseminated chromite is as variable in composition within a thin section as between the MX3 and MX4 sections; the composition probably depends upon very local conditions after initial crystallization. The disseminated chromite varies in diameter between 0.04 and 0.5 mm; no correlation was found between the diameter of the grains and the compositional parameters shown in Figures 3 and 4. The disseminated chromite is consistently higher in $Fe^{2+}/(Fe^{2+} + Mg)$ than the chromite in chromitite, which probably reflects both reaction with intercumulus melt and subsolidus equilibration with nearby silicates (Irvine 1967). The disseminated chromite has higher $Fe^{3+}/(Fe^{3+} + Al + Cr)$, Ti and Ni, whereas the average $Cr/(Cr + Al)$ is similar to that of the chromite in the chromitite. The average $Cr/(Cr + Al)$ is relatively constant across the half-meter interval shown in Figures 3 and 4, but is more variable in disseminated chromite. The $Fe^{3+}/(Fe^{3+} + Al + Cr)$ and amount of Ti and Ni in disseminated chromite show a pronounced increase with stratigraphic height above the main chromitite band in both MX3 and MX4.

The range in composition of the chromite in chromitite and disseminated chromite is also shown on Figures 17 and 18. The disseminated chromite has a higher $Fe^{2+}/(Fe^{2+} + Mg)$ and $Fe^{3+} + 2Ti$ than the chromite in chromitite. The disseminated chromite that is in contact with very fine-grained, irregular intergrowths of chlorite and alkali feldspar, or less commonly, albite, is generally higher in $Cr/(Cr + Al)$ (open triangles in Figs. 17, 18). Some of the disseminated chromite (open circles in Figs. 17, 18) that is in contact with, or included within, what appear to be olivine relics now altered to a mixture of talc and serpentine (Fig. 5), has a lower $Cr/(Cr + Al)$ than most of the disseminated chromite.

DISCUSSION

The processes that contributed to the evolution of the chromitite in the Muskox intrusion can be grouped into three general categories: 1) primary cumulus crystallization of olivine, orthopyroxene and chromite, 2) modification in the magmatic environment, 3) post-magmatic alteration. These are equivalent to the cumulus, postcumulus and subsolidus stages used by Cameron (1975) to describe the evolution of chromite and silicates in the Bushveld Complex.

The appearance of chromitite in layered basic intrusions is fairly common; however, the chromitite in the Muskox intrusion is unique in that it occurs relatively high up in the stratigraphic section (Fig. 2). The two chromitite horizons in the Muskox are in a cyclic unit, with peridotite at the base, followed by chromitite, orthopyroxenite, websterite and, in the case of cyclic unit 22, by gabbro. The rock types found in our study are consistent with the identification by Irvine & Smith (1967) of peridotite grading to orthopyroxenite; however, at the small scale of the present study, there is no obvious boundary between these rock types. Indeed, at this scale, it might be better

TABLE 1. COMPOSITION OF MINERALS ASSOCIATED WITH CHROMITITE IN THE MUSKOX COMPLEX

	1.	2.	3.	4.	5.	6.	7.	8.	9.	10.	11.	12.	13.	14.	15.	16.
	Opx.	Opx.	Cpx.	Cpx.	Ol.	Tlc.+Srp.	Ilm.	Bt.	Ilm.	Hem.	Bt.	Chr.	Rt.	Arm.	Ilm.	Pl.
Slide	MX332B	MX414A	MX303A	MX303	MX303	MX332B	MX332B	MX332B	MX323	MX323	MX323	MX408A	MX408A	MX408A	MX408A	MX408A
Loc.			core	rim	Fig. 13		Fig. 13	Fig. 13	Fig. 15	Fig. 15	Fig. 15	Fig. 16	Fig. 16	Fig. 16	Fig. 16	
SiO_2	55.24	55.10	52.51	51.64	37.73	54.25	0.35	38.78	0.16	1.45	38.33	0.21	0.25	0.18	0.19	54.06
TiO_2	0.21	0	0.66	0.81	0	0	47.85	2.06	48.99	0.33	6.84	5.89	95.54	66.31	52.07	0.12
Al_2O_3	0.48	0.82	2.09	2.44	0	1.53	0.22	15.30	0.09	0.21	12.74	4.80	0.06	1.15	0.16	28.92
Cr_2O_3	0	0.07	0.97	0.75	0	0.15	0.56	0	0.60	0	0.37	29.27	1.10	7.57	1.22	0.09
FeOT	15.45	14.57	6.78	6.80	24.82	9.22	46.71	12.47	45.15	90.30	9.49	53.91	0.37	16.27	40.34	0.45
MnO	0.36	0.25	0	0.27	0.35	0.29	0.53	0.11	0.36	0	0.10	0.19	0	0.15	0.38	0
MgO	28.75	28.91	16.28	16.24	37.59	24.40	3.55	16.22	4.27	0.35	17.70	3.85	0	1.92	4.73	0.15
CaO	0.47	0.47	21.04	20.88	0.15	0.81	0	3.45	0	0	0.13	0.08	0.22	3.93	0.06	11.37
Na_2O	0	0	0.52	0.38	0	0	0	1.51	0	0	0.72	0.12	0	0.21	0	4.48
K_2O	0	0	0	0	0	0.08	0	6.29	0	0.05	9.29	0	0	0.03	0	0.59
SUM	100.96	100.19	100.55	100.21	100.64	90.73	99.77	96.19	99.62	92.69	95.71	98.32	97.54	97.72	99.15	100.23
Si^4	7.881	7.885	7.677	7.624	5.930	8.313	0.069	6.14	0.032	0.335	6.090	0.045	0.042	0.033	0.038	7.327
Ti^4	0.023	0.000	0.073	0.090	0.000	0.000	7.036	0.246	7.188	0.058	0.818	0.941	11.799	9.058	7.672	0.012
Al^3	0.081	0.139	0.363	0.425	0.000	0.277	0.051	2.85	0.021	0.058	2.386	1.202	0.012	0.247	0.037	4.619
Fe^3	0.000	0.000	0.000	0.000	0.000	0.000	1.725	0.000	1.481	11.596	0.000	3.927	0.000	0.000	0.383	0.000
Cr^3	0.000	0.008	0.113	0.088	0.000	0.019	0.087	0.000	0.093	0.000	0.047	4.916	0.143	1.088	0..189	0.010
Fe^2	1.844	1.744	0.834	0.840	3.263	1.182	5.914	1.652	5.887	5.821	1.261	5.651	0.051	2.472	6.228	0.051
Mn^2	0.044	0.031	0.000	0.034	0.047	0.038	0.088	0.015	0.060	0.000	0.014	0.035	0.000	0.024	0.064	0.000
Mg^2	6.114	6.166	3.568	3.574	8.806	5.573	1.035	3.828	1.242	0.121	4.192	1.219	0.000	0.520	1.382	0.030
Ca^2	0.072	0.073	3.315	3.303	0.026	0.133	0.000	0.586	0.000	0.000	0.023	0.019	0.039	0.765	0.013	1.651
Na^1	0.000	0.000	0.149	0.109	0.000	0.000	0.000	0.464	0.000	0.000	0.222	0.050	0.000	0.074	0.000	1.202
K^1	0.000	0.000	0.000	0.000	0.000	0.016	0.000	1.271	0.000	0.015	1.883	0.000	0.000	0.007	0.000	0.102

The analytical results are reported in weight % oxides and cations per 24 oxygen ions. FeOT: total Fe expressed as FeO. Arm: armalcolite. Loc.: Figure showing the grains that were analyzed.

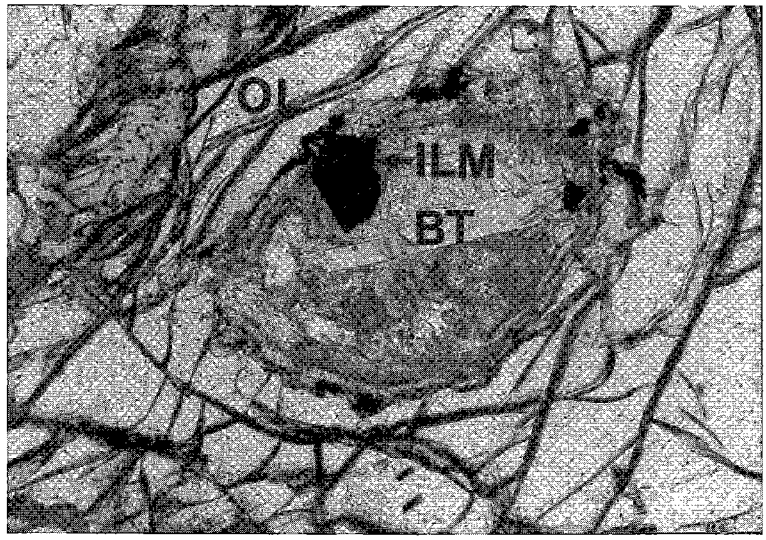

FIG. 13. Enlarged view of pocket of accessory minerals in olivine (OL) indicated by arrow in Figure 12. The minerals include biotite (BT), ilmenite (ILM), serpentine, chlorite, clinopyroxene and sulfide. This is considered to have been the location of a pocket of late intercumulus melt. See Table 1 (Nos. 5, 7, 8) for the composition of the labeled minerals. Slide MX–332B (depth 126–132 cm). Width of field of view: 0.9 mm.

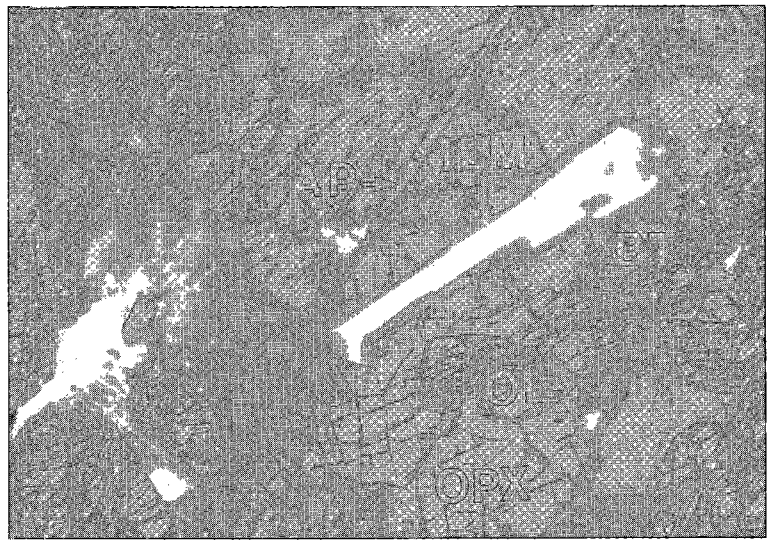

FIG. 14. Orthopyroxenite with olivine (OL), Ilmenite (ILM), biotite (BT), plates of hematite in biotite and an acicular crystal of apatite (AP). Slide MX–323 (depth 85–89 cm). Width of field of view: 6.7 mm.

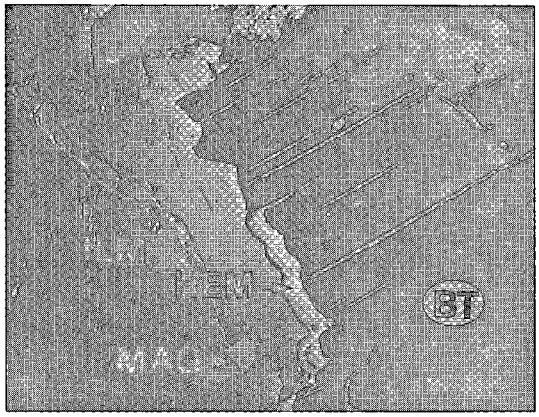

FIG. 15. Back-scattered electron image of part of the large grain of ilmenite in Figure 14. The minerals include ilmenite (ILM), biotite (BT), chromian magnetite (MAG), sulfide (top center) and plates of hematite (HEM) extending from the ilmenite into the biotite. See Table 1 (Nos. 9, 10, 11) for the composition of some of the labeled minerals. Slide MX–323 (depth 85–89 cm). Width of field of view: 0.5 mm.

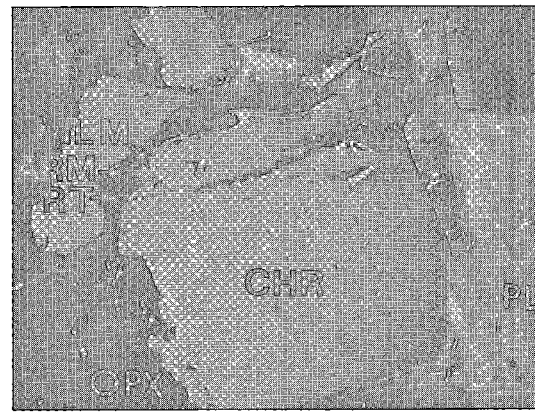

FIG. 16. Back-scattered electron image of a large crystal of chromite (CHR) in plagioclase (PL) and orthopyroxene (OPX). See Table 1 (Nos. 13, 14, 15) for the composition of the labeled rutile (RT), armalcolite (ARM) and ilmenite (ILM). Slide MX–408A (depth 19–22 cm). Width of field of view: 0.4 mm.

to describe these rocks as orthopyroxenites, with varying amounts of olivine, that include a band of chromitite 10 cm thick and a few thin wispy bands of chromitite. The interpretation of cumulus *versus* intercumulus phases is fraught with danger (Jackson 1961, Irvine 1982); however, our interpretation of the textures is consistent with that of Irvine & Smith (1967). We have identified three cumulus, or primary crystalline phases; olivine, orthopyroxene and chromite. Postcumulus processes in the presence of melt have changed the

TABLE 2. REPRESENTATIVE COMPOSITIONS OF CHROMITE ASSOCIATED WITH CHROMITITE IN THE MUSKOX COMPLEX

	1	2	3	4	5	6	7	8	9	10	11	12	13	14
Samp.	MX-3	MX-3	MX-3	MX-3	MX-3	MX-3	MX-3	MX-4	MX-4	MX-4	MX-4	MX-4	MX-4	MX-4
	Diss.	Diss.	Diss.	Seam	Seam	Seam	Diss.	Diss.	Diss.	Diss.	Diss.	Seam	Seam	Seam
Depth	0.3	8.3	14.3	29.1	29.9	33.0	37.5	4.3	9.6	14.1	18.9	33.1	34.2	35.7
SiO_2	0.60	0.71	0.56	0.38	0.40	0.53	0.30	0.25	0.26	0.26	0.32	0.53	0.28	0.48
TiO_2	8.55	4.27	7.18	3.59	3.68	3.55	3.79	9.91	7.65	5.41	3.40	3.49	3.63	3.32
Al_2O_3	5.60	3.55	7.73	12.80	12.38	12.35	15.61	6.58	8.26	11.19	3.98	10.89	11.61	10.66
Cr_2O_3	17.95	34.50	26.31	36.08	36.37	36.46	26.60	22.09	27.35	25.49	31.42	37.40	37.29	39.57
FeO	60.91	54.38	51.51	38.38	38.93	39.12	45.81	54.70	49.36	50.73	57.81	37.41	37.88	37.42
MnO	0.36	0.52	0.33	0	0.05	0.19	0.74	0.70	0.96	0.38	0.50	0.16	0.13	0.24
MgO	4.60	2.10	5.51	7.66	7.51	7.55	5.38	5.39	5.41	4.92	0.90	7.22	7.32	7.31
CaO	0.08	0.08	0.10	0.15	0.20	0.23	0.25	0.11	0.05	0.18	0.28	0.22	0.18	0.26
NiO	0.55	0.59	0.35	0.42	0.49	0.39	0.44	0.54	0.48	0.60	0.51	0.35	0.33	0.29
ZnO	0.16	0	0.06	0	0.08	0.17	0.24	0	0.24	0.09	0.07	0.08	0.09	0.19
V_2O_3	0.61	0.81	0.58	0.60	0.63	0.61	0.46	0.67	0.66	0.65	0.91	0.51	0.59	0.54
SUM	99.97	101.51	100.22	100.16	100.70	101.15	99.62	100.94	100.68	99.85	100.10	98.26	99.33	100.28
Si^4	0.021	0.025	0.02	0.013	0.014	0.018	0.010	0.009	0.009	0.009	0.012	0.018	0.010	0.016
Ti^4	0.222	0.113	0.184	0.089	0.091	0.088	0.095	0.253	0.195	0.138	0.092	0.089	0.092	0.083
Al^3	0.228	0.147	0.310	0.497	0.479	0.476	0.609	0.264	0.330	0.445	0.168	0.434	0.457	0.418
Fe^3	0.808	0.632	0.587	0.360	0.367	0.377	0.483	0.612	0.525	0.576	0.722	0.358	0.351	0.347
Cr^3	0.490	0.956	0.707	0.939	0.944	0.942	0.696	0.593	0.732	0.680	0.888	1.000	0.985	1.040
Fe^2	0.948	0.962	0.877	0.697	0.701	0.692	0.785	0.942	0.872	0.856	1.005	0.701	0.707	0.694
Mn^2	0.011	0.016	0.010	0	0.002	0.006	0.210	0.021	0.028	0.011	0.016	0.005	0.004	0.007
Mg^2	0.237	0.11	0.279	0.376	0.368	0.368	0.266	0.273	0.273	0.248	0.048	0.364	0.365	0.362
Ca^2	0.003	0.004	0.004	0.006	0.008	0.009	0.009	0.004	0.002	0.007	0.011	0.008	0.007	0.010
Ni^2	0.016	0.017	0.01	0.012	0.013	0.011	0.012	0.015	0.014	0.017	0.015	0.010	0.009	0.008
Zn^2	0.005	0	0.002	0	0.002	0.005	0.006	0	0.006	0.003	0.002	0.002	0.003	0.005
V^3	0.017	0.023	0.016	0.016	0.017	0.016	0.013	0.019	0.018	0.017	0.027	0.014	0.016	0.015
FE^2#	0.800	0.898	0.759	0.650	0.656	0.653	0.747	0.775	0.762	0.776	0.954	0.658	0.660	0.657
CR#	0.683	0.867	0.695	0.654	0.663	0.664	0.533	0.693	0.690	0.604	0.841	0.697	0.683	0.713

The analytical results are reported in weight % oxides and cations per 4 oxygen ions. Depth is expressed in cm in the MX-3 or MX-4 stratigraphic section. Chromite is either from chromitite seam or disseminated (Diss.). $FE^2\# = Fe^{2+}/(Fe^{2+} + Mg)$. $CR\# = Cr/(Cr + Al)$.

morphology of all three phases, with the volume proportion of olivine having decreased by reaction and the formation of both postcumulus orthopyroxene and clinopyroxene at the expense of olivine and melt. The phases, textural associations and sequence of crystallization in these Muskox samples are very similar to those described for other intrusions (Jackson 1961, 1970, Roeder & Campbell 1985, Hulbert & Von Gruenewaldt 1985).

The very low solubility of chromium in silicate melts (Roeder & Reynolds 1991) probably means that there has been little significant change in the volume proportion of chromite in the chromitite during postcumulus processes. On the other hand, the number of chromite crystals has decreased, and the size of crystals has increased, owing to sintering and recrystallization. The small size and amount of chromite in the remaining olivine and the larger size of chromite grains along silicate grain-boundaries, and of those associated with intercumulus plagioclase, suggest that grain coarsening occurred in the presence of late intercumulus melt. Indeed, in the Muskox chromitite, some of the largest grains of chromite are enclosed by plagioclase. The composition of the chromite in the chromitite does not vary depending on the size of the chromite grains or the type of enclosing silicate. This suggests that the process of grain coarsening did not significantly affect the composition of the chromite in the chromitite.

One method to test whether the minerals that are present have retained the composition at the time of primary magmatic crystallization is to see whether these compositions can be used to calculate a reasonable set of initial conditions (Irvine 1975). Irvine (1967) suggested that in order to test the conditions of initial magmatic crystallization of chromite, olivine and pyroxene, it is best to use the composition of the minerals in adjacent units, where they occur at maximum concentration. The average composition of chromite in chromitite is $Cr/(Cr + Al) = 0.681$, $Fe^{2+}/(Fe^{2+} + Mg) = 0.662$ and $Fe^{3+}/(Fe^{3+} + Al + Cr) = 0.205$, and the average olivine in the orthopyroxenite is $Fo_{76.7}$. The 1993 version of the equations described by Sack & Ghiorso (1991) have been used to calculate a temperature of 1146°C at which this chromite and olivine can coexist at equilibrium. The oxygen fugacity has been calculated for the chromite – olivine – orthopyroxene equilibrium using the equations of O'Neill & Wall (1987). The calculated $\log f(O_2)$ is –9.2, which is essentially the same as that for the quartz – fayalite – magnetite buffer [$\log f(O_2) = -9.07$] at 1146°C. There are many assumptions implicit in these calculations, and thus the resulting temperature and oxygen fugacity can be used only as a general guide. We conclude that

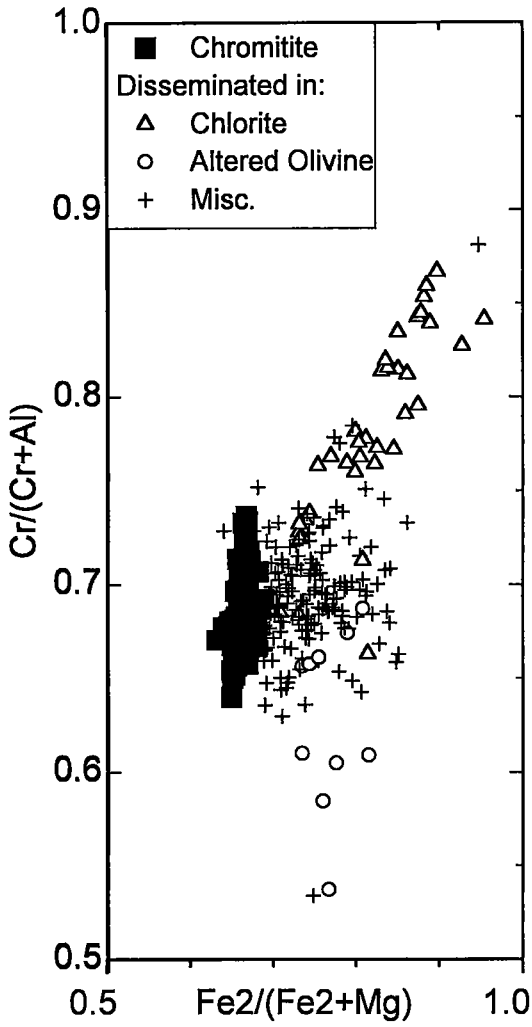

FIG. 17. Cr/(Cr + Al) *versus* $Fe^{2+}/(Fe^{2+} + Mg)$ for disseminated chromite and chromite in chromitite from the Muskox intrusion. The compositions of disseminated chromite have been divided into three categories depending upon the minerals associated with the chromite.

the calculated temperature and oxygen fugacity are reasonable for the primary crystallization of these minerals, as shown by experimental studies (*e.g.*, Roeder & Reynolds 1991).

The composition of chromite in chromitite from the Muskox intrusion, the Bushveld Complex, the Stillwater Complex and the Great Dyke are shown in Figures 19 and 20. The variation in the composition of chromite from these four layered intrusions can be compared in these figures to the general variation in composition shown by the spinel-group minerals (small dots) from various geological environments. These data are taken from the spinel database of twenty-one thousand compositions initially described by Roeder (1994). The Muskox chromite in chromitite has a higher $Fe^{2+}/(Fe^{2+} + Mg)$ and $Fe^{3+} + 2Ti$ than those in the chromitites from the Bushveld, Stillwater and Great Dyke Complexes, but a similar Cr/(Cr + Al). If it is assumed that the composition of the Muskox chromite in the chromitite reflects primary crystallization, then we can conclude that the melt compositions that gave rise to this chromite were more evolved than those of the other intrusions. The most common composition of chromite in the Bushveld chromitite horizons is shown in Figures 19 and 20. Local examples exist, however, where the chromite can become very rich in Fe and Ti (Cameron & Glover 1973, Scoon & Mitchell 1994). Such Fe- and Ti-rich chromite in the Bushveld is usually associated with mafic pegmatites and the pipes that are generally recognized (Merkle 1988) as having formed later than the chromitites by the action of late intercumulus melt (Kinloch & Peyerl 1990, Scoon & Mitchell 1994) or a water-rich fluid (Stumpfl & Rucklidge 1982).

As explained earlier, the chromitite horizons at Muskox are also unique in their relative position so high within the intrusion. Irvine (1979) and Francis (1994) showed how the Mg/(Mg + Fe) for the whole-rock pyroxenite layers in the Muskox go from 0.81 at the base of megacycle 1 to a maximum of 0.87 in megacycle 2 to about 0.76 at the chromitite horizons in megacycle 4. In the opinion of Francis, this trend was produced by a combination of primary magma contaminated in megacycle 1 by the selective melting of the country-rock gneiss and the increasing influence up-section of fractional crystallization of the magma and mixing with new additions of primitive magma. The change from megacycle 2 to megacycle 3 is considered to involve mixing of new magma with fractionated magma within the chamber. By the time that most of megacycle 3 had formed, orthopyroxene became the second silicate phase to crystallize after olivine. This may have been due to a combination of fractional crystallization within the chamber, the addition of new magma and a component of high-silica melted roof-rock. The relatively high $Fe^{2+}/(Fe^{2+} + Mg)$, $Fe^{3+}/(Fe^{3+} + Al + Cr)$ and Ti of the chromite in the Muskox chromitite suggest that the magma was relatively rich in Fe and Ti by the time megacycle 4 crystallized. The very presence of chromitite suggests that much of the chromium was introduced by a new pulse of a more primitive magma. The magma at the time of deposition of the upper portion of megacycle 4 was quite evolved, as shown by the magnetite- and ilmenite-rich oxide layers near the roof (Irvine & Smith 1967).

There have been three models suggested for the formation of the Muskox chromitites. These models were developed mainly to explain the problem of

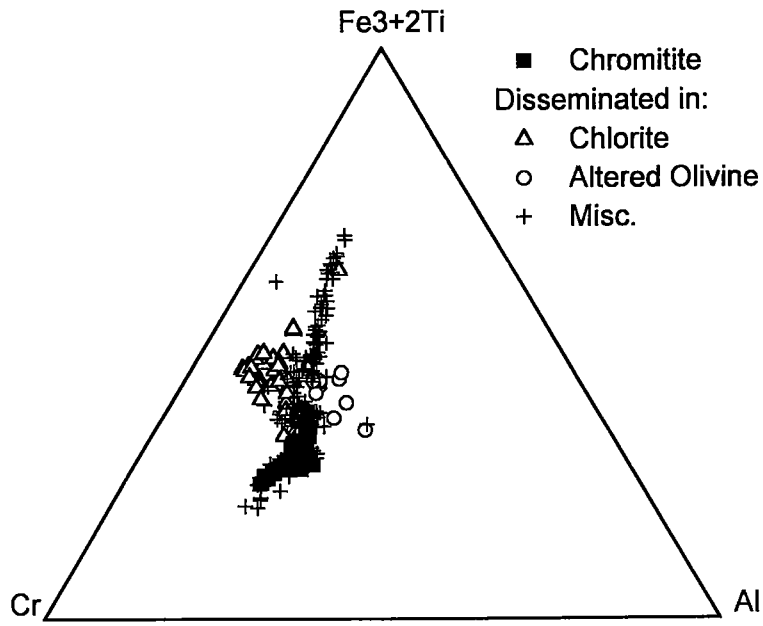

FIG. 18. Composition in terms of Cr – Al – (Fe^{3+} + 2Ti) for disseminated chromite and chromite in chromitite from the Muskox intrusion. The compositions of disseminated chromite have been divided into three categories depending upon the minerals associated with the chromite.

developing a seam of nearly pure chromite that contains little or no cumulus silicates such as olivine or orthopyroxene. Irvine & Smith (1967) suggested that the chromite concentrations were mainly the result of cotectic crystallization of olivine and chromite, followed by a period of little or no crystallization, but differential settling of olivine and chromite. Under these conditions, the small crystals of chromite would settle at a much lower rate and thus could become concentrated above, and separated from, the silicates that accumulated in a lower peridotite layer. Irvine (1974, 1975) suggested a different model that involved the mixing of a new pulse of magma with a roof-contaminated magma. Because of possible curvature of the cotectic between olivine and chromite, this mixed magma was considered to have a composition entirely within the chromite primary phase-field. Irvine used the presence of alkali- and silica-enriched inclusions in chromite in the chromitite as evidence to support this model. Irvine (1977) then suggested that "subsequent work has revealed that this mechanism is probably not adequate". His more viable alternative involves the same curved olivine–chromite cotectic, but the mixing of a more primitive melt with a melt already in the chamber that had evolved by fractional crystallization within the chamber. The evidence from the present study as it bears on these models is not definitive. Francis (1994) suggested that the appearance of orthopyroxene as the third silicate in megacycle 3 and its appearance as the second phase in megacycle 4 coincides with spikes in LIL/HFS element ratios, indicating contamination at the level of the upper crust, as originally suggested by Irvine (1970).

The available evidence is compatible, in our opinion, with a combination of 1) contamination by roof rocks, 2) evolved magma from within the intrusion and, 3) a pulse of new magma to bring more chromium into the chamber and bring olivine back onto the liquidus. The introduction of a new pulse of magma into the chamber at a fairly late stage in the evolution of the Muskox chamber may have meant that the new magma had the opportunity of mixing with both roof-contaminated magma and evolved magma. This could have led to a period of negligible crystallization of silicate and thus concentration of chromite by settling. On the other hand, the small amount of peridotite below the chromitite in cycle 22 does not support this alternative. The detailed modeling of processes within the Muskox intrusion in order to explain the chromitite layers is questionable, specially since the exposed part of the intrusion may be such a small part of the complex (Irvine & Baragar 1972). Thus the scale of the processes that led to the chromitites is largely unknown.

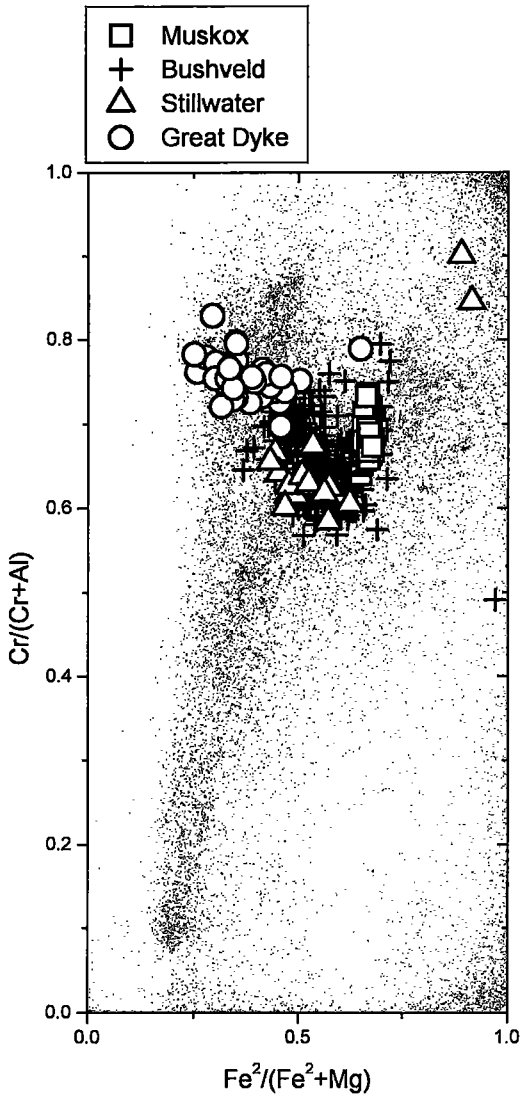

FIG. 19. Cr/(Cr + Al) *versus* $Fe^{2+}/(Fe^{2+} + Mg)$ for chromite in chromitite from: Bushveld intrusion (van de Walt 1941, Cameron & Emerson 1959, Cameron 1964, 1977, de Waal 1975, McLaren & De Villiers 1982, Engelbrecht 1985, Hatton & Von Gruenewaldt 1985, 1987, Eales & Reynolds 1986, Nicholson & Mathez 1991, Scoon & Teigler 1994), Stillwater intrusion (Stevens 1944, Howland 1955, Sampson 1966, Beeson & Jackson 1969, Nicholson & Lipin 1985), the Great Dyke (Worst 1964, Wilson 1982), and the Muskox intrusion (present study). The small dots represent spinel compositions taken from the spinel database initially described by Roeder (1994).

There is significant evidence that late-stage reaction of intercumulus melt with disseminated chromite, and later subsolidus reaction, were responsible for the spread of $Fe^{2+}/(Fe^{2+} + Mg)$, Fe^{3+}, Ti and Ni. The local variability in disseminated chromite and the upward increase in the above compositional parameters for disseminated chromite above the main chromitite band suggest some upward percolation of intercumulus melt. This upward change did not seem to significantly affect the smaller bands of chromitite (Figs. 3, 4). Irvine (1980) described the cyclic change in a number of compositional parameters through the dunite and olivine clinopyroxenite layers of cycles 4–7 near the base of the Muskox layered series. He showed that the base of a cyclic unit commonly represents a sharp modal change, such as olivine clinopyroxenite to dunite, and an increase in modal disseminated chromite. Thus the start of a cyclic unit may represent a new influx of magma into the intrusion. Irvine described how chemical changes such as $Fe^{2+}/(Fe^{2+} + Mg)$ in olivine, and Ni in both olivine and chromite, were displaced meters above modal discontinuities at the base of a cyclic unit. He explained this displacement by a process of infiltration metasomatism where compaction of the cumulates resulted in upward movement of melt and displacement of the chemical changes from the modal discontinuities. The increase in $Fe^{2+}/(Fe^{2+} + Mg)$, $Fe^{3+}/(Fe^{3+} + Al + Cr)$, Ti and Ni in the disseminated chromite above the thickest chromitite in MX–3 and MX–4 is attributed to the same kind of infiltration metasomatism.

The concentration of late interstitial melt in some locations (Figs. 13, 14) gave rise to a complex assemblage of silicates and oxides. The decrease in temperature that caused melt reaction and crystallization may have also caused local re-equilibration in $Fe^{2+}/(Fe^{2+} + Mg)$ of disseminated chromite, olivine and pyroxene. This re-equilibration would have continued to increase the $Fe^{2+}/(Fe^{2+} + Mg)$ of disseminated chromite at subsolidus temperatures by the mechanism described by Irvine (1967). The textural evidence suggests that the last minor phases to crystallize from the melt are plagioclase, biotite and ilmenite. The last remnants of melt are considered to have occupied those sites where there is biotite plus ilmenite, local strong zoning in plagioclase, fine-grained alteration assemblages and, in some instances, a ragged appearance of the orthopyroxene.

Subsolidus alteration seems to have changed the composition of disseminated chromite that is presently associated with chlorite and other hydrothermal minerals. This is distinct from the subsolidus equilibration of $Fe^{2+}/(Fe^{2+} + Mg)$ with olivine and pyroxene that was described above. These chromite grains associated with chlorite may have lost some aluminum during the formation of chlorite, and thus increased the Cr/(Cr + Al) of chromite. This trend is similar to the trend shown by chromite altering to "ferritchromit"

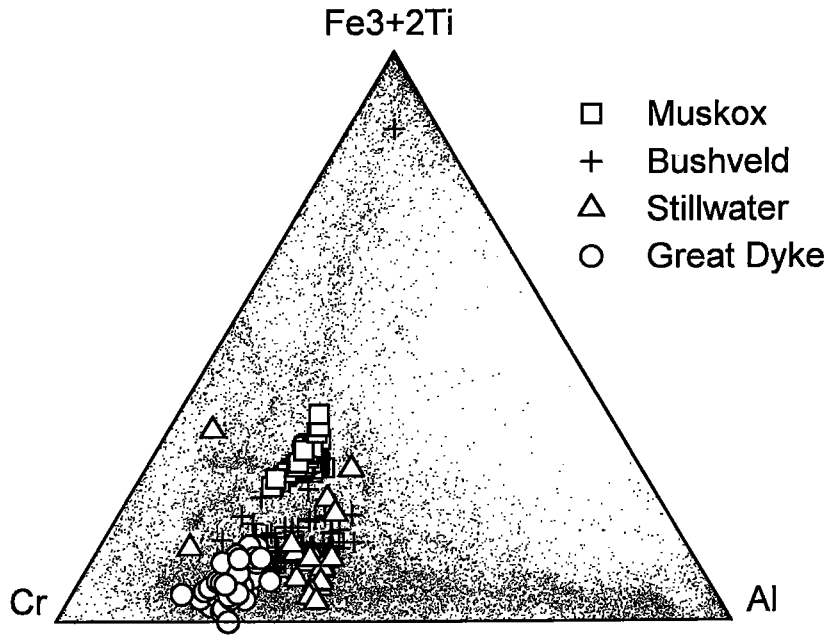

FIG. 20. Composition of chromite in terms of Cr – Al – (Fe^{3+} + 2Ti) for chromite in chromitite from: Bushveld Complex, Stillwater Complex, the Great Dyke, Muskox intrusion and spinel database. See Figure 19 caption for details.

(Roeder 1994). This is only a minor trend for the Muskox disseminated chromite, and no real "ferritchromit" with low Al has been found. The only other subsolidus trend that has been noted, but not explained, is that some chromite associated with altered olivine shows a tendency to have a lower Cr/(Cr + Al).

SUMMARY AND CONCLUSIONS

1) The chromite in two 0.5-m drill cores of the chromitite and orthopyroxenite in cycle 22 of the Muskox intrusive body has been described and analyzed.

2) The chromite in the massive and wispy chromitite bands shows a narrow range in composition, Cr/(Cr + Al) in the range 0.64–0.74, $Fe^{2+}/(Fe^{2+} + Mg)$ in the range 0.62–0.69, and $Fe^{3+}/(Fe^{3+} + Al + Cr)$ in the range 0.18–0.26. The range is the same in the two drill cores.

3) The disseminated chromite in the orthopyroxenite and olivine orthopyroxenite has a higher and more variable $Fe^{2+}/(Fe^{2+} + Mg)$, in the range 0.64–0.95, $Fe^{3+}/(Fe^{3+} + Al + Cr)$ in the range 0.14–0.54, and has a similar, but more variable Cr/(Cr + Al), in the range 0.53–0.88, than the chromite in the chromitite.

4) The $Fe^{2+}/(Fe^{2+} + Mg)$, $Fe^{3+}/(Fe^{3+} + Al + Cr)$, Ti and Ni of the disseminated chromite increases with stratigraphic height above the massive 10-cm seam of chromitite in both drill-core sections. This is explained by infiltration metasomatism of late-intercumulus melt.

5) The texture and oxide mineralogy are described for pockets of minerals, which are considered to have been the location of late-intercumulus melt.

6) The composition of chromite from the Muskox chromitite is compared to the general range in composition of spinel-group minerals, and to the range in composition of chromite from chromitites of the Bushveld Complex, Stillwater Complex and the Great Dyke. The higher $Fe^{2+}/(Fe^{2+} + Mg)$, Fe^{3+} and Ti of the Muskox chromite in chromitite are considered to be due to its formation late in the history of the magma chamber from a magma that combined fractionated magma with roof-contaminated magma and an influx of a more primitive magma.

ACKNOWLEDGEMENTS

We thank Equinox Exploration for making this study possible by donating the drill core from the Muskox intrusion. We also thank David Kempson and Roger Innis for their help with the research, and Joan Charbonneau for her help in preparing the manuscript. Financial support was provided by the Natural Sciences and Engineering Research Council of Canada. We are very grateful to Dogan Paktunc, Grant Cawthorn and Robert F. Martin for reviewing the manuscript.

References

ALBEE, A.L. & RAY, L. (1970): Correction factors for electron microprobe microanalysis of silicates, oxides, carbonates, phosphates and sulphates. *Anal. Chem.* **42**, 1408-1414.

BEESON, M.H. & JACKSON, E.D. (1969): Chemical composition of altered chromites from the Stillwater Complex, Montana. *Am. Mineral.* **54**, 1084-1100.

BENCE, A.E. & ALBEE, A.L. (1968): Empirical correction factors for the electron microanalysis of silicates and oxides. *J. Geol.* **76**, 382-403.

BOWLES, J.F.W. (1988): Definition and range of composition of naturally occurring minerals with the pseudobrookite structure. *Am. Mineral.* **73**, 1377-1383.

CAMERON, E.N. (1964): Chromite deposits of the eastern part of the Bushveld Complex. *In* The Geology of some Ore Deposits in Southern Africa (S.H. Haughton, ed.). *Geol. Soc. S. Afr., Spec. Publ.* **2**, 131-168.

_____ (1975): Postcumulus and subsolidus equilibration of chromite and coexisting silicates in the Eastern Bushveld Complex. *Geochim. Cosmochim. Acta* **39**, 1021-1033.

_____ (1977): Chromite in the central sector of the Eastern Bushveld Complex, South Africa. *Am. Mineral.* **62**, 1082-1096.

_____ & EMERSON, M.E. (1959): The origin of certain chromite deposits of the eastern part of the Bushveld Complex. *Econ. Geol.* **54**, 1151-1213.

_____ & GLOVER, E.D. (1973): Unusual titanian–chromian spinels from the eastern Bushveld Complex. *Am. Mineral.* **58**, 172-188.

CAWTHORN, R.G. & BARRY, S.D. (1992): The role of intercumulus residua in the formation of pegmatoid associated with the UG2 chromite, Bushveld Complex. *Aust. J. Earth Sci.* **39**, 263-276.

_____ & BIGGAR, G.M. (1993): Crystallization of titaniferous chromite, magnesian ilmenite and armalcolite in tholeiitic suites in the Karoo Igneous Province. *Contrib. Mineral. Petrol.* **114**, 221-235.

DESROCHES, V. (1992): *Petrogenesis of the Pyroxenite Units in the Muskox Intrusion.* M.Sc. thesis, McGill Univ., Montreal, Quebec.

DE WAAL, S.A. (1975): The mineralogy, chemistry, and certain aspects of reactivity of chromitite from the Bushveld igneous complex. *National Institute for Metallurgy, South Africa, Rep.* **1709**, 1-80.

EALES, H.V. & REYNOLDS, I.M. (1986): Cryptic variations within chromitites of the Upper Critical Zone, northwestern Bushveld Complex. *Econ. Geol.* **81**, 1056-1066.

ENGELBRECHT, J.P. (1985): The chromites of the Bushveld Complex in the Nietverdiend area. *Econ. Geol.* **80**, 896-910.

FRANCIS, D. (1994): Chemical interaction between picritic magmas and upper crust along the margins of the Muskox intrusion, Northwest Territories. *Geol. Surv. Can., Pap.* **92-12**, 1-94.

HANSKI, E.J. (1992): Petrology of the Pechenga ferropicrites and cogenetic, Ni-bearing gabbro–wehrlite intrusions, Kola Peninsula, Russia. *Geol. Surv. Finland, Bull.* **367**, 1-196.

HATTON, C.J. & VON GRUENEWALDT, G. (1985): Chromite from the Swartkop chrome mine – an estimate of the effects of subsolidus reequilibration. *Econ. Geol.* **80**, 911-924.

_____ & _____ (1987): The geological setting and petrogenesis of the Bushveld chromitite layers. *In* Evolution of Chromium Ore Fields (C.W. Stowe, ed.). Van Nostrand Reinhold, New York, N.Y. (109-143).

HOFFMAN, P.F. (1984): Geology, northern internides of Wopmay Orogen, District of Mackenzie, Northwest Territories. *Geol. Surv. Can., Map* **1576A.**

HOWLAND, A.L. (1955): Chromite deposits in the central part of the Stillwater complex, Sweet Grass County, Montana. *U.S. Geol. Surv., Bull.* **1015-D**, 99-121.

HULBERT, L.J. & VON GRUENEWALDT, G. (1985): Textural and compositional features of chromite in the lower critical zones of the Bushveld Complex south of Potgietersrus. *Econ. Geol.* **80**, 872-895.

IRVINE, T.N. (1967): Chromian spinel as a petrogenetic indicator. 2. Petrologic implications. *Can. J. Earth Sci.* **4**, 71-103.

_____ (1970): Crystallization sequences in the Muskox intrusion and other layered intrusions. 1. Olivine – pyroxene – plagioclase relations. *Geol. Soc. S. Afr., Spec. Publ.* **1**, 441-476.

_____ (1974): Chromitite layers in stratiform intrusions. *Carnegie Inst. Wash., Year Book* **73**, 300-316.

_____ (1975): Crystallization sequences in the Muskox intrusion and other layered intrusions. II. Origin of chromitite layers and similar deposits of other magmatic ores. *Geochim. Cosmochim. Acta* **39**, 991-1020.

_____ (1977): Origin of chromitite layers in the Muskox intrusion and other stratiform intrusions: a new interpretation. *Geology* **5**, 273-277.

_____ (1979): Rocks whose composition is determined by crystal accumulation and sorting. *In* The Evolution of the Igneous Rocks, Fiftieth Anniversary Perspectives (H.S. Yoder, Jr., ed.). Princeton University Press, Princeton, New Jersey (245-306).

_____ (1980): Magmatic infiltration metasomatism, double-diffusive fractional crystallization, and adcumulus growth in the Muskox intrusion and other layered intrusions. *In* Physics of Magmatic Processes (R.B. Hargraves, ed.). Princeton University Press, Princeton, New Jersey (325-384).

_____ (1982): Terminology of layered intrusions. *J. Petrol.* **23**, 127-162.

_____ & BARAGAR, W.R.A. (1972): Muskox intrusion and Coppermine River lavas, Northwest Territories, Canada. *Int. Geol. Congress, Guidebook* (D.J. Glass, ed.), 1-70.

_____ & SMITH, C.H. (1967): The ultramafic rocks of the Muskox intrusion, Northwest Territories, Canada. *In* Ultramafic and Related Rocks (P.J. Wyllie, ed.). John Wiley & Sons, Inc., New York, N.Y. (38-49).

_____ & _____ (1969): Primary oxide minerals in the layered series of the Muskox intrusion. *In* Magmatic Ore Deposits, a Symposium (H.D.B. Wilson, ed.). *Econ. Geol., Monogr.* **4**, 76-94.

JACKSON, E.D. (1961): Primary textures and mineral associations in the ultramafic zone of the Stillwater Complex, Montana. *U.S. Geol. Surv., Prof. Pap.* **358**, 1-106.

_____ (1970): The cyclic unit in layered intrusions – a comparison of repetitive stratigraphy in the ultramafic parts of the Stillwater, Muskox, Great Dyke, and Bushveld Complexes. *Geol. Soc. S. Afr., Spec. Publ.* **1**, 391-424.

KINLOCH, E.D. & PEYERL, W. (1990): Platinum-group minerals in various rock types of the Merensky reef: genetic implications. *Econ. Geol.* **85**, 537-555.

LECHEMINANT, A.N. & HEAMAN, L.M. (1989): Mackenzie igneous events, Canada: Middle Proterozoic hotspot magmatism associated with ocean opening. *Earth Planet. Sci. Lett.* **96**, 38-48.

MCLAREN, C.H. & DE VILLIERS, J.P.R. (1982): The platinum-group chemistry and mineralogy of the UG-2 chromitite layer of the Bushveld Complex. *Econ. Geol.* **77**, 1348-1366.

MERKLE, R.K.W. (1988): The effects of metasomatising fluids on the PGE-content of the UG-1 chromitite layer. *In* Geo-Platinum 87 (H.M. Prichard, P.J. Potts, J.F.W. Bowles and S.J. Cribb, eds.). Elsevier, London, U.K. (359).

NICHOLSON, D.M. & MATHEZ, E.A. (1991): Petrogenesis of the Merensky Reef in the Rustenburg section of the Bushveld Complex. *Contrib. Mineral. Petrol.* **107**, 293-309.

NICHOLSON, S.W. & LIPIN, B.R. (1985): Guide to the Gish Mine area. *In* The Stillwater Complex, Montana; Geology and Guide (G.K. Czamanske & M.L. Zientek, eds.). *Montana Bureau of Mines and Geology, Spec. Publ.* **92**, 358-367.

O'NEILL, H.ST.C. & WALL, V.J. (1987): The olivine – orthopyroxene – spinel geothermometer, the nickel precipitation curve, and the oxygen fugacity of the Earth's upper mantle. *J. Petrol.* **28**, 1169-1191.

ROACH, T.A. (1992): *Formation and Evolution of the Main Chromitite, Muskox Layered Intrusion, Northwest Territories.* M.Sc. thesis, Queen's Univ., Kingston, Ontario.

ROEDER, P.L. (1994): Chromite: from the fiery rain of chondrules to the Kilauea Iki lava lake. *Can. Mineral.* **32**, 729-746.

_____ & CAMPBELL, I.H. (1985): The effect of postcumulus reactions on composition of chrome-spinels from the Jimberlana intrusion. *J. Petrol.* **26**, 763-786.

_____ & REYNOLDS, I. (1991): Crystallization of chromite and chromium solubility in basaltic melts. *J. Petrol.* **32**, 909-934.

SACK, R.O. & GHIORSO, M.S. (1991): Chromian spinels as petrogenetic indicators: thermodynamics and petrological applications. *Am. Mineral.* **76**, 827-847.

SAMPSON, E. (1966): Discussion – Stillwater, Montana chromite deposits. *In* Magmatic Ore Deposits, a Symposium (H.D.B. Wilson, ed.). *Econ. Geol., Monogr.* **4**, 72-75.

SCOON, R.N. & MITCHELL, A.A. (1994): Discordant iron-rich ultramafic pegmatites in the Bushveld Complex and their relationship to iron-rich intercumulus and residual liquids. *J. Petrol.* **35**, 881-917.

_____ & TEIGLER, B. (1994): Platinum-group element mineralization in the Critical Zone of the Western Bushveld Complex. I. Sulfide poor-chromitites below the UG-2. *Econ. Geol.* **89**, 1094-1121.

SMITH, C.H. (1962): Notes on the Muskox intrusion, Coppermine River area, District of MacKenzie. *Geol. Surv. Can., Pap.* **61-25**, 1-16.

_____, IRVINE, T.N. & FINDLAY, D.C. (1963): Geology of the Muskox intrusion. *Geol. Surv. Can., Maps* **1213A**, **1214A**.

STEVENS, R.E. (1944): Composition of some chromites of the Western Hemisphere. *Am. Mineral.* **29**, 1-34.

STUMPFL, E.F. & RUCKLIDGE, J.C. (1982): The platiniferous dunite pipes of the eastern Bushveld. *Econ. Geol.* **77**, 1419-1431.

VAN DER WALT, C.F.J. (1941): Chrome ores of the Western Bushveld Complex. *Trans. Geol. Soc. S. Afr.* **44**, 79-112.

WILSON, A.H. (1982): The geology of the Great "Dyke", Zimbabwe: the ultramafic rocks. *J. Petrol.* **23**, 240-292.

WORDEN, R.H., DROOP, G.T.R. & CHAMPNESS, P.E. (1991): The reaction antigorite → olivine + talc + H_2O in the Bergell aureole, N. Italy. *Mineral. Mag.* **55**, 367-377.

WORST, B.G. (1964): Chromite in the Great Dyke of Southern Rhodesia. *In* The Geology of Some Ore Deposits in southern Africa (S.H. Haughton, ed.). The Geological Society of South Africa, Johannesburg, South Africa (209-224).

Received August 14, 1995, revised manuscript accepted November 29, 1997.